SUPPORTING INFORMATION

Abnormal cannabidiol modulates vitamin A metabolism by acting as a competitive inhibitor of CRBP1

Josie A. Silvaroli[1#], Made Airanthi K. Widjaja-Adhi[1#], Thomas Trischman[1], Sylwia Chelstowska[1], Samantha Horwitz[1,2], Surajit Banerjee[3,4], Philip D. Kiser[1,5,6], William S. Blaner[7], and Marcin Golczak[1,6]

From the: [1]Department of Pharmacology, School of Medicine, Case Western Reserve University, Cleveland, OH; [2]Kent State University, Kent, OH; [3]Department of Chemistry and Chemical Biology, Cornell University, Ithaca, NY; [4]Northeastern Collaborative Access Team, Argonne National Laboratory, Argonne, IL; [5]Research Service, Louis Stokes Cleveland VA Medical Center, Cleveland, OH; [6]Cleveland Center for Membrane and Structural Biology, School of Medicine, Case Western Reserve University, Cleveland, OH; [7]Department of Medicine, College of Physicians and Surgeons, Columbia University, New York, NY

[#]These authors contributed equal to this study.

To whom the correspondence should be addressed: Marcin Golczak, Ph.D., Department of Pharmacology, School of Medicine, Case Western Reserve University, 10900 Euclid Ave, Cleveland, Ohio 44106, USA; Phone: 216–368–0302; Fax: 216–368–1300; E–mail: mxg149@case.edu.

Supporting Information Table 1 – The K_i values for the interaction of abn-CBD, its selected derivatives, and vitamin A with CRBP1

Ligand	K_i (nM) Δ fluorescence at 350 nm	K_i (nM) Δ fluorescence at 480 nm
abn-CBD[1]	66.7 ± 6.7	76.3 ± 8.5
abn-CBDO[1]	285.0 ± 16.0	236.3 ± 22.9
CBDO[1]	1,786.5 ± 161.0	1,662.0 ± 258.3
O-1918[1]	>> 10,000	>> 10,000
limonene[1]	n.d.[3]	n.d.
all-*trans*-retinol[2]	33.8 ± 2.7	36.4 ± 2.5

[1] Determined in all-*trans*-retinol-replacement assay

[2] Determined by replacement of abn-CBD by all-*trans*-retinol from the binding site of CRBP1

[3] n.d. – not detectable

Supporting Information Table 2 – X-ray data collection and refinement statistics

Protein **Ligand**	**CRBP1** **abn-CBD**	**CRBP1** **abn-CBDO**	**CRBP1** **CBDO**	**CRBP3** **abn-CBD**	**CRBP4** **abn-CBD**
PDB code	6E5L	6E5T	6E6M	6E5W	6E6K
Beam line	24-ID-C	BL9-2	24-ID-C	24-ID-C	BL9-2
Wavelength (Å)	0.9791	0.9795	0.9791	0.9791	0.9795
Data collection					
Space group	$P2_12_12_1$	$P2_12_12_1$	$P2_12_12_1$	$P2_12_12_1$	$C121$
Cell dimensions					
a, *b*, *c* (Å)	37.22, 40.89, 92.14	37.32, 40.74, 92.08	37.21, 93.03, 119.84	37.46, 127.51, 160.23	35.04, 57.39, 67.99
α, β, γ (°)	90.00, 90.00, 90.00	90.00, 90.00, 90.00	90.00, 90.00, 90.00	90.00, 90.00, 90.00	90.00, 103.67, 90.00
Resolution (Å)	46.07-1.17[1] (1.19-1.17)[2]	46.04-1.55[1] (1.58-1.55)[2]	73.49-1.55[1] (1.58-1.55)[2]	99.77-2.50[1] (2.60-2.50)[2]	33.03-1.30[1] (1.32-1.30)[2]
R_{sym} (%)	11.9 (59.6)[2]	9.2 (82.9)[2]	8.9 (80.2)[2]	17.3 (86.8)[2]	11.0 (70.8)[2]
R_{pim} (%)	5.2 (31.2)[2]	3.9 (35.7)[2]	5.5 (48.2)[2]	8.2 (43.4)[2]	7.3 (48.8)[2]
$I/\sigma I$	11.6 (5.5)[2]	12.8 (2.9)[2]	9.0 (2.6)[2]	7.2 (2.7)[2]	7.7 (2.3)[2]
CC(1/2)	0.99 (0.69)[2]	1.00 (0.66)[2]	1.00 (0.85)[2]	0.99 (0.80)[2]	0.99 (0.47)[2]
Completeness (%)	99.3 (99.5)[2]	99.2 (99.5)[2]	100 (100)[2]	99.9 (99.9)[2]	95.0 (96.3)[2]
Redundancy	5.8 (4.8)[2]	11.9 (11.9)[2]	6.5 (6.7)[2]	5.8 (5.3)[2]	6.1 (5.9)[2]
Refinement					
Resolution (Å)	46.07-1.17	34.57-1.55	73.49-1.55	99.77-2.50	33.03-1.30
No. of reflections	47,869	20,856	61,150	27,415	30,514
R_{work}/R_{free} (%)	11.8/14.6	17.6/22.4	16.6/20.3	18.9/23.8	16.9/19.5
No. of atoms	1,555	1,463	4,340	4,738	1,418
Protein	1,230	1,202	3,521	4,405	1,144
Ligand	23 (HVD)[3]	19 (HVJ)[3]	57 (8CB)[3]	92 (HVD)[3] 24 (GOL)[3]	23 (HVD)[3]
Water	302	242	762	217	281
Mean *B*-factor (Å^2)					
Protein	11.2	23.7	18.8	30.3	12.2
Ligand	11.9 (HVD)[3]	25.3 (HVJ)[3]	20.8 (8CB)[3]	43.5 (HVD)[3] 37.5 (GOL)[3]	15.8 (HVD)[3]
Water	28.2	34.5	33.5	32.3	27.1
R.m.s. deviations					
Bond lengths (Å)	0.007	0.009	0.009	0.012	0.008
Bond angles (°)	0.916	1.042	1.002	1.239	0.960
Validation					
Ramachandran					
Favored/outliers (%)	98.6/0	98.6/0	97.6/0	98.3/0	98.5/0
Rotamer outliers (%)	0	1.5	0	1.4	0
Clash score	0.4	1.2	2.5	1.6	2.7

[1]Data set was collected on a single crystal

[2]Highest-resolution shell is shown in parentheses

[3]Ligand identifier code

Supporting Information Figure 1

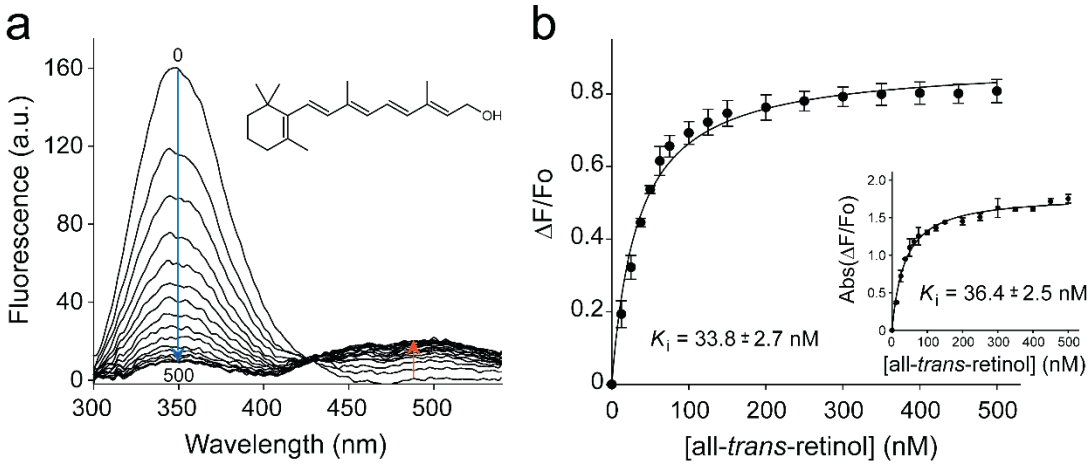

Replacement of abn-CBD from the binding site of CRBP1 by vitamin A. **a**, Changes in the fluorescence spectra of the CRBP1/abn-CBD complex upon titration with all-*trans*-retinol. **b**, Determination of the K_i value for vitamin A interaction. Changes in the emission maxima at 350 nm and 480 nm (inset) were plotted versus concentration of vitamin A and fitted to the one site saturation ligand binding model (R_{sqr} = 0.990 and 0.986 for the fluorescence signal at 350 nm and 480 nm, respectively). The experiments were repeated three separate times, each time in duplicate. Data are presented as mean values of the six runs ± sd.

Supporting Information Figure 2

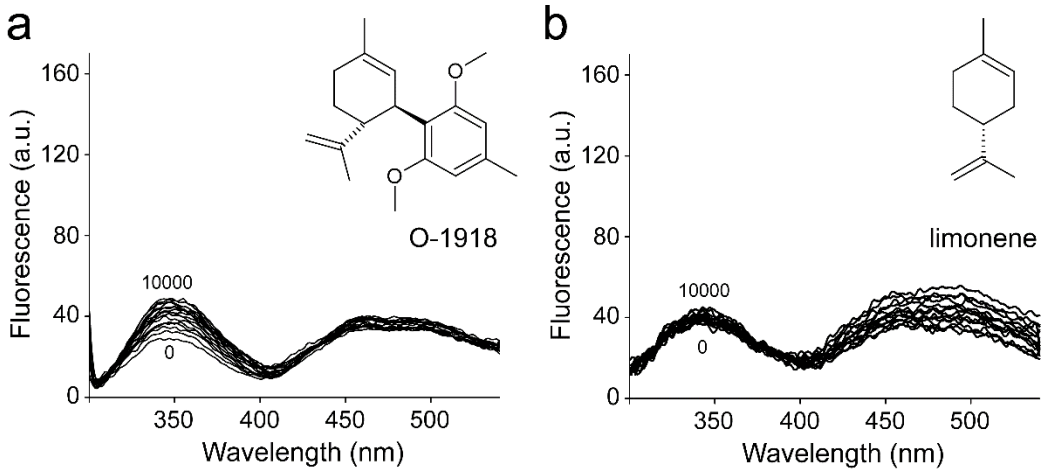

The lack of interactions of selected abn-CBD derivatives with CRBP1. Titration of holo-CRBP1 with derivatives of abn-CBD, O-1918 or limonene (panels **a** and **b**, respectively) did not reveal meaningful changes in the fluorescence properties of the protein/vitamin A complex, indicating the lack of significant affinity for tested compound for CRBP1. The measurements were performed in the concentration range between 0 and 10,000 nM. The experiments were repeated three times in duplicate. Data are presented as mean values of six runs ± sd.

Supporting Information Figure 3

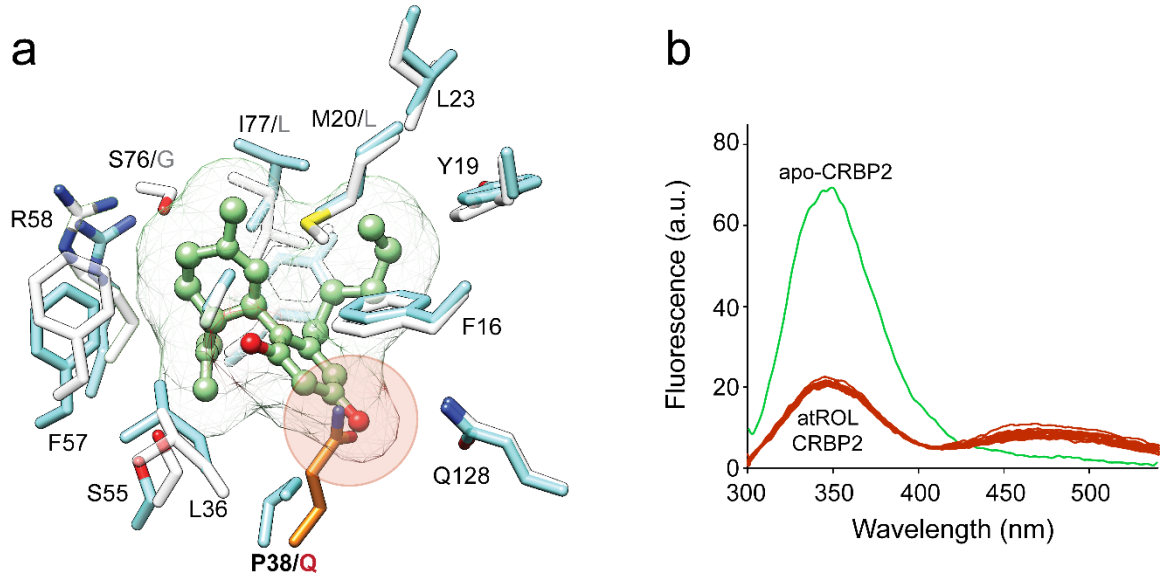

Structural basis for the inability of abn-CBD to interact with CRBP2. **a**, Close-up view of the ligand binding site of superimposed structures of CRBP1 (light blue) in complex with abn-CBD (green) and CRBP2 colored grey (PDB # 6E5L and 6BTI, respectively). A side chain of a glutamine residue (colored orange) that substitutes P38 in CRBP1 protrudes into the binding cavity abolishing interaction of CRBP2 with abn-CBD. The area of potential clashes is indicated by an orange circle. **b**, The structural prediction was confirmed experimentally by titration of holo-CRBP2 with abn-CBD in the concentration range between 0 – 5,000 nM (red traces). The absence of changes in the fluorescence spectra (increase of signal at 350 nm and decrease at 480 nm) indicates the inability of abn-CBD to replace all-*trans*-retinol in the protein's binding pocket. A reference fluorescence spectrum of apo-CRBP2 is shown in green.

Supporting Information Figure 4

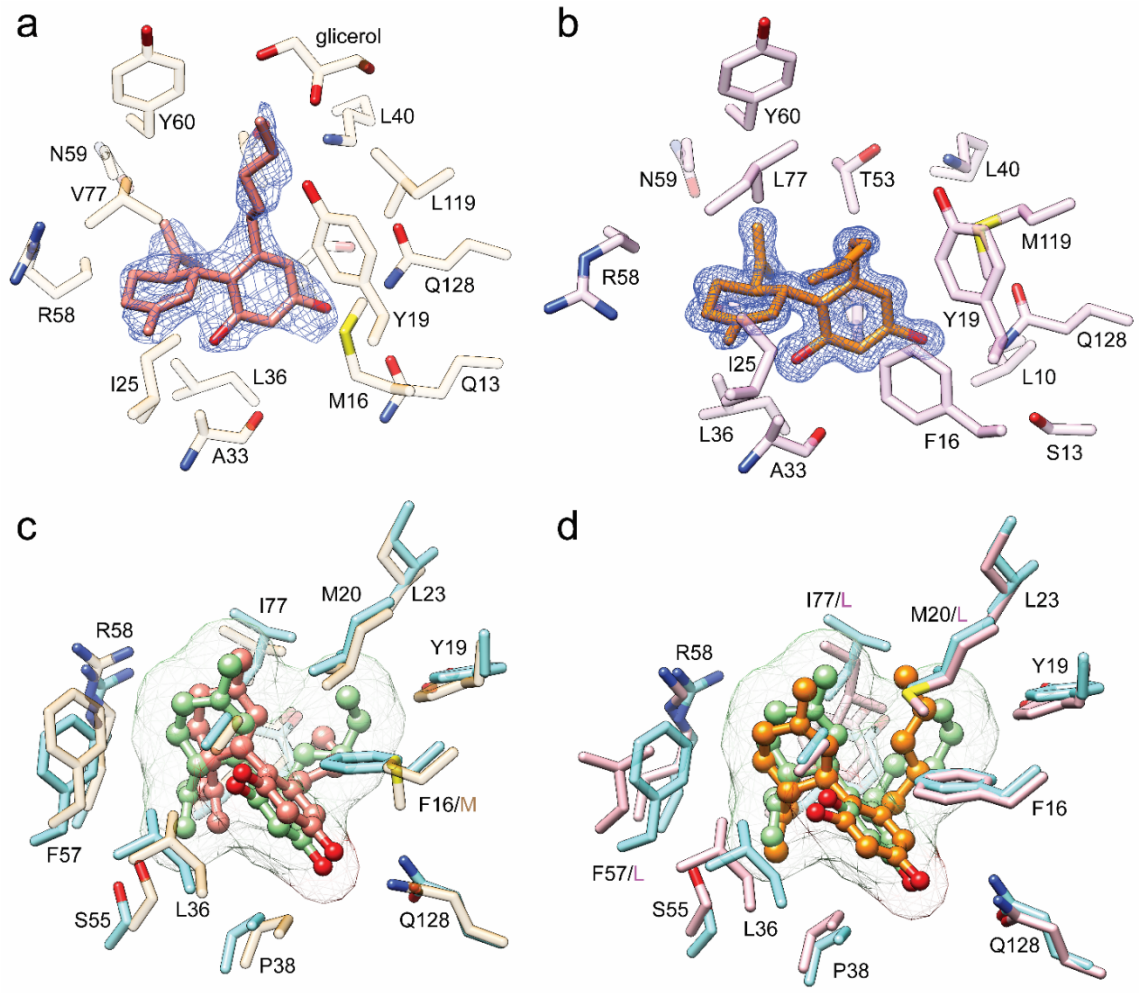

Structural basis for the abn-CBD's binding to CRBP3 and CRBP4. Panels **a**, and **b** represent electron density maps for abn-CBD bound to CRBP3 and CBRP4, respectively (PDB # 6E5W and 6E6K). The blue meshes correspond to the $2F_o - F_c$ electron density maps, contoured at 1.2σ for both structures. **c**, Close-up view of the ligand binding site of superimposed structures of CRBP1 (light blue) and CRBP3 (beige) (PDB # 6E5Land 6E5W, respectively) in complex with abn-CBD. **d**, Overlay of CRBP1 structures (light blue) with CRBP4 (light purple, PDB # 6E6K) bound to abn-CBD. Although there are several differences in the amino acids composition, they do not contribute to a dramatic alteration of the architecture or the polarity of the binding sites. Thus, the overall orientations and the mode of the protein-ligand interactions are very similar in the examined structures.

Supporting Information Figure 5

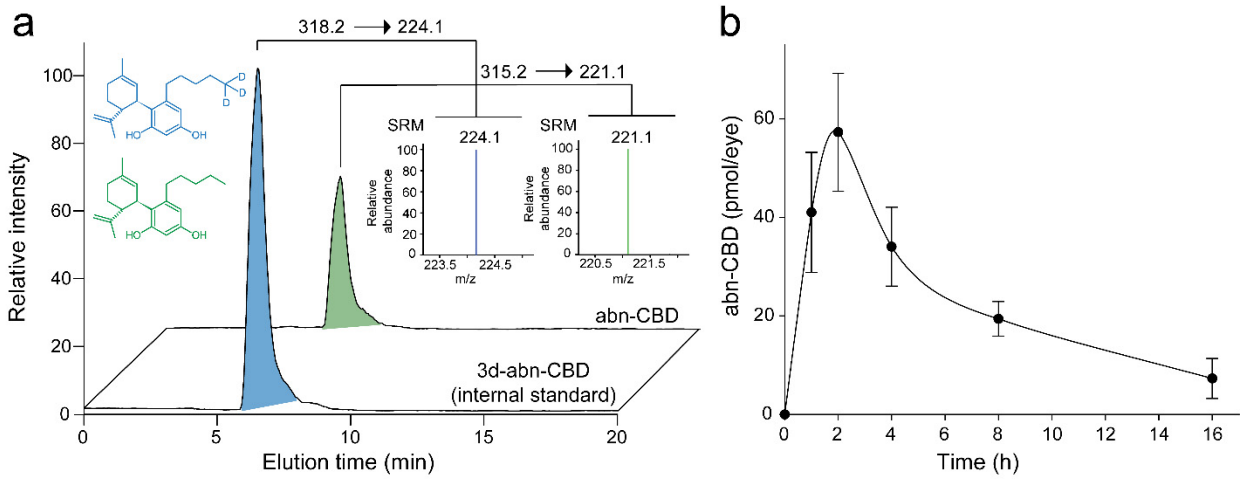

Detection and quantification of abn-CBD in mouse eye. **a**, Extracted ion chromatograms for abn-CBD (m/z = 315.2 $[MH]^+$) and its deuterated form (3d-abn-CBD) at m/z = 318.2 $[MH]^+$ which served as an internal standard for the quantification purpose. The insets show the fragmentation patterns for these parent ions. Characteristic fragmentation profiles were used to design the selected reaction monitoring-based detection and quantification method. **b**, Pharmacokinetic profile of abn-CBD in the eye after i.p. injection of 250 µg per mouse.

Supporting Information Figure 6

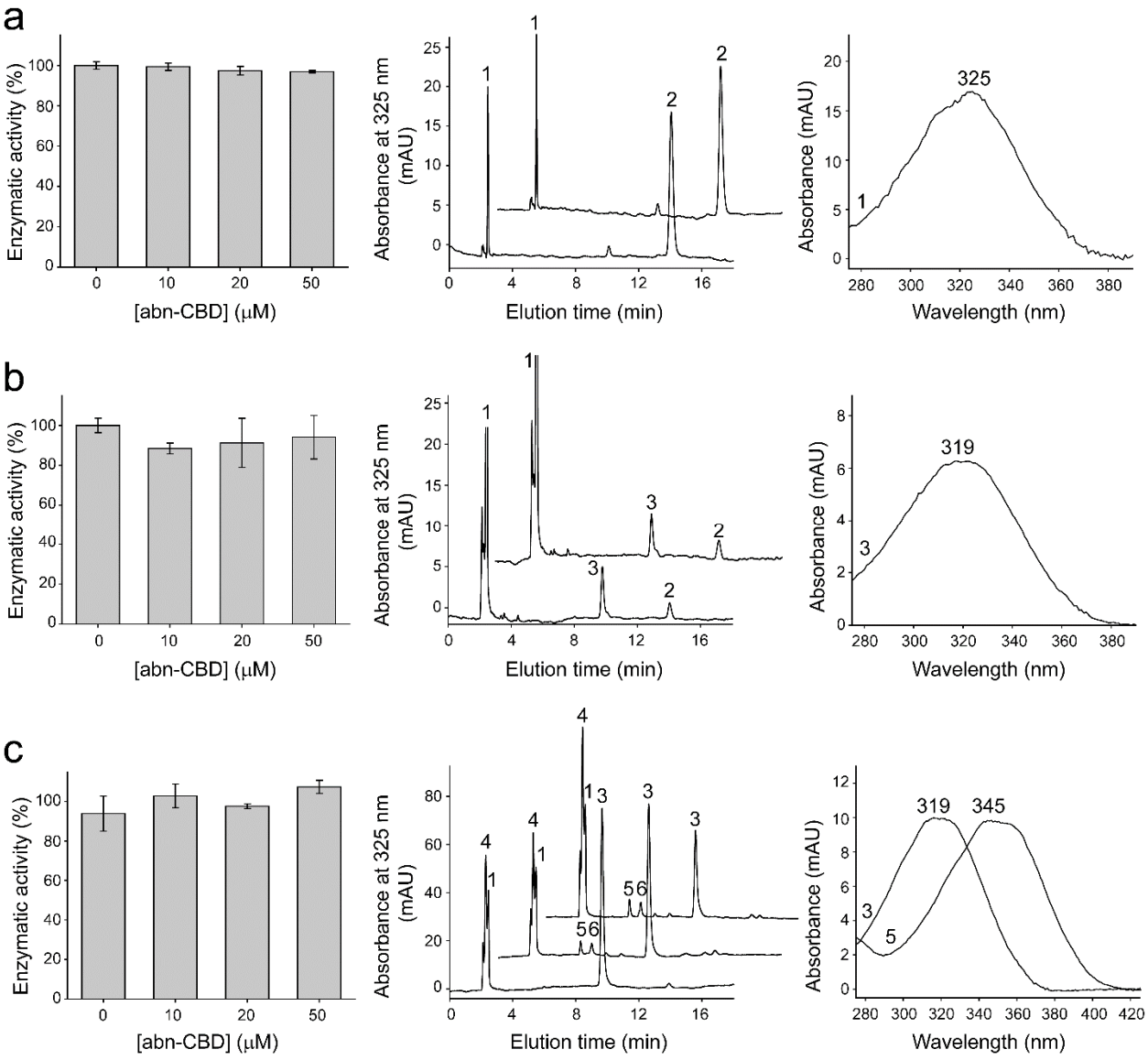

Evaluation of the effect of abn-CBD on the activities of key enzymes of the visual cycle. Bovine RPE microsomes were pre-incubated with 10 – 50 μM of abn- CBD for 5 min at room temperature prior to the addition of retinoid substrates to the final concentration of 10 μM. The initial rates of the enzymatic reactions were measured as described in the material and methods section. Retinoids were extracted with hexane, separated and quantified by normal phase HPLC. **a**, The effect of abn-CBD on lecithin:retinol acyltransferase (LRAT) activity. An excess of tested compound did not inhibit

esterification of all-*trans*-retinol. The peaks shown in the representative chromatograms correspond to:1 – all-*trans*-retinyl esters (products); 2 – all-*trans*-retinol (substrate). The right panel represents a UV/Vis spectrum for the chromatographic peak 1. **b**, RPE65-dependent retinoid isomerization activity was not affected by abn-CBD. Analogous to panel **a**, chromatographic peaks 1 and 2 correspond to all-*trans*-retinyl esters and 2 – all-*trans*-retinol (substrate), respectively. Peak 3 indicates the product of isomerization, 11-*cis*-retinol, whose characteristic UV/Vis spectrum is shown in the right panel. **c**, The enzymatic activity of microsomal retinol dehydrogenases (RDHs) in the presence of abn-CBD. The measurements were done for the reduction of 11-*cis*-retinol into a corresponding 11-*cis*-retinal. The data indicated the lack of interference of the tested cannabinoid with cis-RDHs activity. The chromatographic peaks 1, 2, and 3 are as described in panels **a** and **b**. Peaks 4, 5, and 6 correspond to 11-*cis*-retinyl esters, syn 11-*cis*-retinal oxime (product), syn all-*trans*-retinal oxime, respectively. The spectra represent 11-*cis*-retinol (λ_{max} at 319 nm) and 11-*cis*-retinal oxime (λ_{max} at 345 nm).

Supporting Information Figure 7

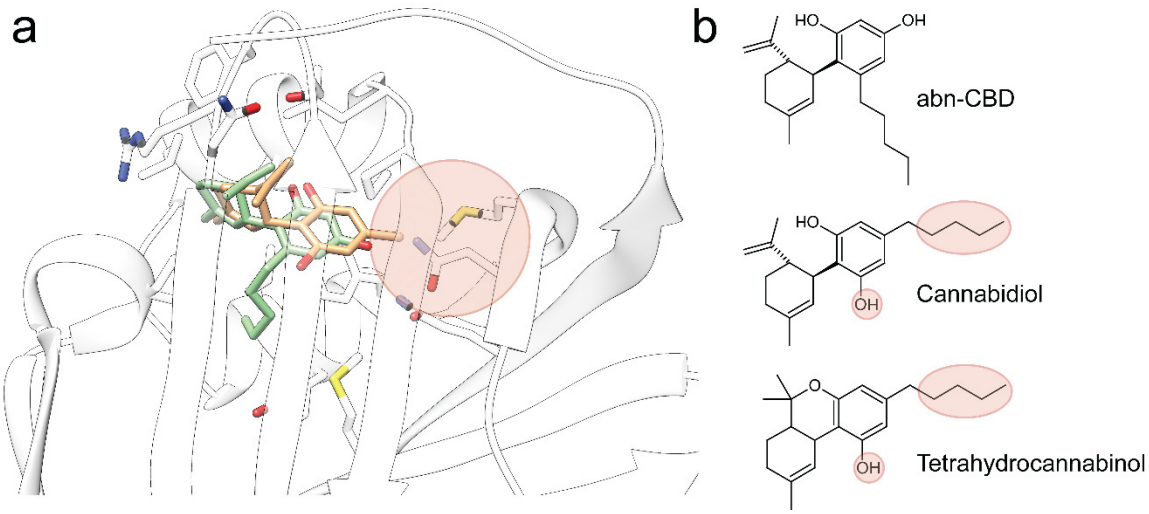

Structural information provides clues about the interaction of cannabidiol and tetrahydrocannabinol with CRBP1. **a**, Comparison of the spatial position of abn-CBD (green) and CBDO (orange) in the binding site of CRBP1. Orientation of CBDO suggests that binding of cannabidiol and tetrahydrocannabinol with reasonable affinity is implausible. These compounds lack the key hydroxyl group in the preferable position, but more importantly their pentyl aliphatic chains cannot be accommodated inside the binding pocket without causing collisions with the protein backbone (marked with orange oval). **b**, Comparison of structures of abn-CBD and the major naturally occurring cannabinoids. Parts of the compounds that make binding to CRBP1 unlikely to bind as compared to abn-CBD are indicated with orange backgrounds.